

PHYSICS IN COLLISION - Stanford, California, June 20-22, 2002

COSMOLOGY: RECENT AND FUTURE DEVELOPMENTS

Joshua A. Frieman

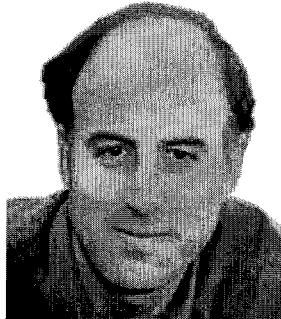
NASA/Fermilab Astrophysics Center

Fermi National Accelerator Laboratory, Batavia, Illinois, USA

and

Department of Astronomy & Astrophysics and Center for Cosmological Physics

The University of Chicago, Chicago, Illinois, USA



ABSTRACT

The precision with which the cosmological parameters have been determined has made dramatic progress in just the last two years. I review this recent observational progress, highlight some of the key questions facing cosmology in the new millennium, and briefly discuss some of the projects now being mounted or contemplated to address them.

1 Introduction: Precision Cosmology

Our knowledge of the cosmological parameters has made tremendous strides in the last two years. We now know that the cosmic baryon density, measured as a fraction of the critical density for a spatially flat Universe, is $\Omega_b = 0.04$, to an accuracy of about 20% (here and below, $\Omega_i = \rho_i/\rho_{crit}$, where the critical density $\rho_{crit} = 3H_0^2/8\pi G$ and H_0 is the present value of the Hubble parameter—the expansion rate of the Universe). (Here and throughout, 1σ errors are quoted.) The density of non-relativistic matter, including baryons and non-baryonic dark matter, is $\Omega_m = 0.3$, again with a precision of about 20%. The density of dark energy, a negative-pressure component responsible for the acceleration of the Universe, is $\Omega_{DE} = 0.7$ to about 15%, and the total density $\Omega_{total} = 1$ to a precision of about 5%. The Hubble parameter $H_0 = 70$ km/sec/Mpc, to an accuracy of about 10%, and the age of the Universe $t_0 = 14$ Gyr, within about 8%. Finally, the slope of the primordial mass density power spectrum—which determines how large-scale structure forms—is $n_s = d \ln P(k)/d \ln k = 1$ to within 10%. In the last few years, the uncertainty in these parameters has dropped from the neighborhood of 50-100% to 10-20%. Moreover, the prospects for improving the precision of the measurement of many of these parameters in the near future are excellent. Equally important, we now have confidence that these determinations are robust, because they derive from independent measurements using different techniques, each with their own systematic errors. This is a relatively new phenomenon in cosmology.

Of particular relevance for this audience is the fact that these now well-established ingredients of the standard cosmological model—non-baryonic dark matter, dark energy, and primordial perturbations from inflation (or some as yet undiscovered alternative thereto)—all require and thus provide evidence for new physics beyond the standard model of particle physics.

2 Structure Formation and Cosmology

Many of the recent advances in cosmological parameter measurement have been made possible by the establishment of a plausible paradigm for the formation of large-scale structure. One can think of this paradigm as a cookbook, with a set of recipes which each differ slightly in their ingredients and instructions. For each recipe, the first step is to specify the ‘initial conditions’, that is, the primordial power spectrum of density fluctuations, based on a theory for the origin of density perturbations in the early Universe. For a number of years, inflation has been

the serious contender here—quantum fluctuations of the inflation field as it rolls down its potential generate a nearly scale-invariant spectrum of adiabatic, usually Gaussian fluctuations in the gravitational potential—though there may be other possibilities. In the second step, we cook with gravity: the initial perturbations grow by gravitational instability to form structure. The gravity oven has knobs which allow us to set the amounts of cold (or hot or warm) dark matter—these impact the relative growth of perturbations on different scales—and the amount and kind of dark energy, which slows the growth rate of perturbations at late times. Finally, we season the Universe with a few baryons and let the whole thing cook.

After about 400,000 years, when protons and electrons recombine to form neutral Hydrogen, the Cosmic Microwave Background (CMB) photons decouple and thereafter travel freely. As a result, the CMB anisotropy to first approximation gives us a snapshot of this last scattering epoch. Since the typical temperature fluctuation amplitude is about 10^{-5} , these anisotropies are well-described by linear perturbation theory, making the CMB an especially clean cosmological probe.

After a few billion years, peering into the oven we see galaxies, clusters, and larger structures form in a hierarchical pattern. Within galaxies, some of the baryonic gas cools and fragments into stars, which release energy and metals when they subsequently explode. Supermassive black holes form in the cores of many young galaxies, powering intense radiation which we see as quasars. At 14 Gyr, we take the Universe out of the oven and compare it to the real thing; if it doesn't taste exactly like the observed Universe, we start over with one of the variation recipes, e.g., by tweaking the inflation model (the initial perturbation spectrum) or the amounts and kinds of dark matter and dark energy. At the present, this gravitational cooking is modelled with N-body simulations augmented by hydrodynamics for the baryon gas. While the simulations have gotten increasingly accurate as computing power has exploded, they are still a long way from having the necessary resolution and spectral range to precisely model all the gravitational and non-gravitational processes that go into producing luminous galaxies. That is, the leap from non-linear gravity to galaxies with stars and hot gas is still one which involves at best educated guesses.

Despite the continuing challenge of modelling all the details of galaxy formation, the structure formation paradigm is nevertheless robust enough that it allows us to probe the cosmological parameters in new ways. The recent data from CMB anisotropies and from large-scale structure are consistent with a recipe that includes about 28% cold dark matter, 68% dark energy, and 4% baryons, with a nearly scale-invariant spectrum of primordial, adiabatic density perturbations. Confidence

in this paradigm was recently bolstered by the first detection of CMB polarization by the DASI experiment (announced after PIC '02) at the level expected [1]. At the same time, one should heed the caveat that the parameter determinations derived from the CMB and large-scale structure are complex, because the physical observables depend typically on a large number of cosmological parameters with varying degrees of degeneracy. Quoted values for a given cosmological parameter therefore rely on marginalizing over other parameters (e.g., the slope n_s , the contribution of tensor modes to the large-angle CMB anisotropy, the optical depth for reionization, etc.) and the priors placed on them.

3 The Baryon Density of the Universe

An example of recent progress is the baryon density of the Universe. Traditionally, the primary probe of the cosmic baryon density has been big bang nucleosynthesis (BBN): the abundances of the light elements ^4He , ^3He , ^7Li , and especially D depend sensitively on the baryon density Ω_b . Recent determinations of the Deuterium abundance in quasar absorption line systems, $D/H = 3 - 4 \times 10^{-5}$, have provided a strong constraint on the baryon density, $\Omega_b h^2 = 0.020 \pm 0.001$, where $h = H_0/100$ km/sec/Mpc [2]. For $h = 0.72 \pm 0.08$, as the Hubble Key Project indicates [3], this implies a cosmic baryon density of about 4% of the critical density. The abundances of ^4He and ^7Li are consistent with this value for Ω_b , but they are not as constraining.

In 2001, the situation changed dramatically: the pattern of anisotropies in the cosmic microwave background (CMB) was measured with unprecedented precision on degree angular scales by three experiments, DASI [4], Boomerang [5], and Maxima [6], providing for the first time an independent determination of Ω_b . The CMB temperature pattern on the sky can be expanded in spherical harmonics $Y_{\ell,m}$. On degree angular scales and below ($\ell > 100$ or so), the CMB angular power spectrum reflects conditions in the baryon-photon fluid around the time of atomic hydrogen recombination [7]. Before recombination, the two components of this fluid are strongly coupled by Compton scattering in the ionized plasma; after this time, the photons and baryons are essentially decoupled. In an overdense perturbation, gravity causes the fluid to compress, while the photon-baryon pressure causes it to expand. A series of acoustic oscillations ensue, and these are imprinted as a series of peaks and troughs in the CMB angular power spectrum as a function of ℓ . Modes at the point of maximum compression at the time when the photons last scatter correspond to the odd-order (first, third,...) peaks, while those at maximum rarefaction lead to the even-order (second, fourth,...) peaks. Since a larger baryon

density increases the inertia of the fluid, it leads to higher amplitude compressional (odd-order) peaks and lower even-order peaks in the CMB power spectrum. By measuring the relative heights of the first two acoustic peaks (in particular, detecting the second peak for the first time), these CMB experiments were able to constrain the baryon density to $\Omega_b h^2 = 0.022 \pm 0.002$ [8, 9]. This result is in remarkable agreement with the BBN determination of the baryon density, yet it is based on completely independent physical effects and subject to different systematic errors. These measurements mutually reinforce our confidence that we understand how the Universe was evolving about one minute and 400,000 years after the Big Bang. In the next few years, measurement of the large-scale galaxy power spectrum should provide a third input on the baryon density: the same acoustic oscillations seen in the CMB should be imprinted in the spatial power spectrum of galaxies, although with much smaller relative amplitude due to the predominance of dark matter over baryons.

4 Ω_{tot} and the Spatial Geometry of the Universe

While the heights of the CMB acoustic peaks are sensitive to the baryon density, the position of the first peak—that is, the characteristic angular size of hot and cold spots in the CMB sky—is sensitive to the spatial geometry of the Universe. The *physical* size of these spots is set by the ‘sound horizon’ at the epoch of last scattering, roughly the distance an acoustic baryon-photon wave has travelled up to that time; this scale is roughly independent of geometry. By contrast, the angular size subtended by these spots depends on the spatial curvature: in a closed universe (positive curvature, $\Omega_{tot} > 1$), photon trajectories from opposite sides of a spot are focused at the observer, so it appears to have a larger angular size than in a flat universe; in an open universe (negative curvature, $\Omega_{tot} < 1$), the spot appears smaller than in a flat Universe. The CMB angular power spectrum determined by DASI, Boomerang, and Maxima yield $\Omega_{tot} = 1.0 \pm 0.03$ [8], consistent with flat spatial sections. This constitutes the first precision measurement of the total density of the Universe, and the first concrete evidence that the Universe is very nearly flat. This result is consistent with the expectation from inflation, which generally predicts that the Universe should be flat at the $\sim 10^{-4}$ level.

These CMB measurements also constrain the shape of the primordial power spectrum to be $n_s = 0.99 \pm 0.05$, [8] (here assuming n_s is constant) again in agreement with the predictions of inflation, in which the spectrum is generally close to scale-invariant ($n_s = 1$).

These CMB measurements have been recently augmented with results from the CBI experiment [10], an interferometer sited on the Atacama plateau in Chile. On angular scales $\ell \sim 200 - 1000$, the CBI results are consistent with previous measurements; in addition, CBI has provided the first measurements of the CMB power spectrum at smaller angular scales, up to $\ell \sim 3500$. For scales $\ell < 2000$, CBI sees a decline in power with decreasing angular size, as expected from viscosity of the photon-baryon fluid (Silk damping) and from the finite thickness of the last-scattering surface; on these scales, the amplitude is in complete agreement with that expected from the earlier experiments. However, on smaller angular scales, $\ell > 2000$, CBI detects excess power over that expected from the CMB, at roughly the 3σ level. One possible explanation (assuming that foreground point sources have been properly subtracted from the signal) is that the excess power is due to the Sunyaev-Zel'dovich (SZ) effect—Compton scattering of the CMB photons by hot gas in galaxy clusters. Simulations indicate that this explanation requires a rather high value for the normalization of the mass power spectrum: the rms mass fluctuations in spheres of radius $8h^{-1}$ Mpc must be $\sigma_8 \sim 1 - 1.1$ [11]. This is somewhat higher than some other measures of the power spectrum amplitude from the abundance of galaxy clusters, which appear to favor $\sigma_8 \sim 0.6 - 0.8$ for the fiducial values of the other cosmological parameters. In any case, for the SZ effect the CMB power spectrum amplitude scales as σ_8^7 ; in principle, therefore, measurement of the CMB on these small scales could provide an interesting probe of the mass power spectrum amplitude. In practice, to date there is not precise agreement about the calibration of the SZ amplitude between different N-body simulations.

While spatial flatness and near scale-invariance of the power spectrum provide strong circumstantial evidence for inflation, they are not necessarily unique predictions of inflation—in principle, there may be other theoretical possibilities for generating both of these features of the observed universe. One possible way of helping distinguish between inflation and other alternatives, and of discriminating among inflation models themselves, lies in the detection of the ‘B-modes’ of CMB polarization generated by primordial gravitational waves (tensor mode fluctuations) [12]. With the recent first detection of CMB polarization [1], this goal is one step closer. However, the B-mode contribution to the polarization signal is expected to be quite small, and there is likely contamination from polarized foregrounds and from weak lensing of the CMB. It is hoped, however, that experiments with sufficient sensitivity to detect polarization B-modes may be mounted over the coming decade.

5 Probes of the Matter Density: Dark Matter & Ω_m

So far we have discussed the baryon density and the total density of the Universe. A third critical ingredient for cosmology is the cosmic density of matter (including baryons and non-baryonic dark matter), Ω_m . While the evidence for dark matter originated with studies of the dynamics of galaxies and galaxy clusters, in recent years a number of new probes of the dark matter density have been employed.

The height of the first acoustic peak in the CMB angular power spectrum is sensitive to the ‘physical’ matter density, $\Omega_m h^2$. Marginalizing over other parameters, the recent experiments yield $\Omega_m h^2 = 0.17 \pm 0.02$ [9], assuming a flat Universe and reasonable priors on other parameters. In the near future, the accuracy of this measurement should improve significantly: the MAP satellite, launched in 2001 by NASA, will probe the CMB power spectrum up to $\ell \sim 1000$ with unprecedented precision, by making an all-sky CMB map with angular resolution of a few arcminutes. MAP is scheduled to release its first year results in January 2003. When completed, MAP should determine $\Omega_m h^2$ with a precision of about 5%, i.e., to better than ± 0.01 using similar priors as above [13]. The Planck satellite, scheduled for launch in ~ 2008 , will provide an all-sky map with even greater resolution and sensitivity and is projected to determine $\Omega_m h^2$ to a precision of ± 0.003 , assuming both temperature and polarization information are available.

Another recent probe of the matter density is the shape of the large-scale power spectrum probed by galaxy surveys. The galaxy power spectrum can be written schematically as $P_g(k) = b_g(k)P_i(k)T(k, P_i(k'))$. Here, the primordial spectrum P_i is determined, e.g., by inflation, and is usually approximated by a power-law, $P_i \sim k^{n_s}$, though in more complicated models it may contain features. The transfer function T is determined by the amounts and kinds of matter in the Universe and depends principally on Ω_m , Ω_b , and h if the dark matter is cold (and additionally on particle masses if there is a hot (i.e., massive neutrino) or warm dark matter component). In linear perturbation theory, when the amplitude of density fluctuations is small, different Fourier modes evolve independently, in which case $T = T(k)$, with $T \rightarrow 1$ on large scales and $T \rightarrow k^{-3}$ asymptotically on small scales (large k). In the non-linear regime, modes with different wavenumbers are coupled, so the non-linear transfer function depends to some extent on the primordial spectrum. The bias factor b_g accounts for the fact that luminous galaxies do not precisely trace the underlying mass distribution. On large scales (say, $1/k > \text{few } h^{-1} \text{ Mpc}$ or so), b_g is expected to be nearly scale-independent, and it appears that optically-selected galaxies are approximately unbiased on these scales frieman12,verde,lahav.

On smaller scales, in the fiducial dark energy+CDM model described above, these galaxies must be anti-biased, $b < 1$, to account for the observed power-law behavior of the two-point galaxy correlation function. In addition, the bias factor is known empirically to be a function of galaxy type: galaxies with different luminosities and colors are observed to have different clustering amplitudes [17, 18]. Finally, to infer the real-space power spectrum from a redshift survey, one must account for the effects of redshift distortions due to peculiar velocities.

In practice, these caveats are usually dealt with by attempting to restrict the cosmological parameter extraction from galaxy surveys to large scales, where the effects of non-linear processing are minimal and bias and redshift distortions are thought to be simple. In this case, the power spectrum amplitude is usually characterized by the *linear theory* σ_8 . The shape of $P(k)$ is determined primarily by $\Omega_m h$, since this combination determines the horizon size at the epoch of matter-radiation equality, the scale below which the transfer function $T(k)$ turns down from unity. (In addition, the power spectrum on small scales is suppressed by increasing Ω_b or the masses of light neutrinos or by decreasing n_s .) Based on the first 160,000 out of 250,000 galaxy redshifts, the recently completed 2dF survey found $\Omega_m h = 0.20 \pm 0.03$ [19] from the shape of the galaxy power spectrum on large scales. The Sloan Digital Sky Survey (SDSS) will measure about 600,000 galaxy redshifts by June 2005 and will obtain 5-band CCD photometry for about 60 million galaxies (a large fraction of them with approximate photometric redshifts). Based on a small sample of about 1.5 million galaxy images from commissioning data, the SDSS found $\Omega_m h = 0.19 \pm 0.04$ [20], with consistent results from a redshift sample of about 30,000 galaxies [18]. Currently, much larger imaging samples with photometric redshifts are under analysis, as is a spectroscopic (redshift) sample of about 170,000 galaxies. These constraints from galaxy surveys are broadly consistent with those from the CMB.

As noted above, the power spectrum measured in a redshift survey differs from the real-space power spectrum, because the radial coordinate in such a survey is recession velocity rather than distance. As a result, the redshift-space clustering is ‘polluted’ by peculiar (non-Hubble flow) velocities. On the other hand, such peculiar velocities are produced by the perturbed density field itself and therefore carry information about the matter content of the Universe. Performing a multipole expansion of the power spectrum (or of the two-point correlation function), on large scales (in the linear regime) the ratio of the quadrupole to monopole moment is determined by the quantity $\beta = \Omega_m^{0.6}/b_g$. For the 2dF survey, Peacock, et al. [21] found $\beta = 0.43 \pm 0.07$, again consistent with $\Omega_m \simeq 0.3$. Another approach to β

involves comparison of the velocity and (galaxy) density fields: this is only practical in the local Universe, where peculiar radial velocities can be inferred via scaling relations from the measurement of galaxy rotation velocities (for spirals) or velocity dispersions (for ellipticals). Unfortunately, the results obtained have depended on which of several methods is used [22] Recently, however, consistent values using two methods on the same sample were obtained, yielding β between 0.51 and 0.57 [23]. Given the errors, this is marginally consistent with the results from redshift distortions.

In the last two years, weak gravitational lensing by large-scale structure has been detected and is now being developed as a probe of the mass power spectrum [24, 25, 26, 27, 28, 29]. Weak lensing is the distortion and amplification of distant galaxy images due to foreground mass concentrations along the line of sight. Like the CMB, it has the advantage that it probes the gravitational potential directly, without relying on biased tracers of the mass. On the downside, the lensing-induced distortion signal is typically smaller than systematic image distortions due to telescope tracking, atmospheric refraction, wind, imperfect optics, etc. In practice, one measures the shapes (second moments) of a very large number of faint source galaxies in deep CCD images and ‘corrects’ them for systematic effects using stellar images in the same field. The corrected galaxy ellipticities provide an estimate of the cosmic shear as a function of angular position. If the source galaxy redshifts are known (or can be sufficiently constrained), the two-point angular correlation function (or smoothed variance or other second-order statistic) of the shear provides an estimate of the foreground mass power spectrum. Several groups have measured such statistics over the range $\sim 1 - 30$ arcmin and have used the results to obtain constraints in the $\sigma_8 - \Omega_m$ plane. The quantity constrained is approximately $\sigma_8(\Omega_m/0.3)^{0.6}$; of the groups reporting results in the last year, some find a value of about 0.95, while others obtain about 0.7, each with errors of about ± 0.15 . Note that there are still significant concerns over the level of systematic errors seen in these measurements. A number of larger weak lensing surveys are on-going (e.g., the Deep Lens Survey, and the CFHT Legacy Survey), and other more ambitious surveys are planned (PANSTARRS, VISTA, LSST, and SNAP).

Galaxy-galaxy lensing is another manifestation of weak lensing which provides a constraint on Ω_m . Here, one correlates the shear of background source galaxies with the positions of foreground ‘lens’ galaxies; in essence, one is measuring the mean shear profile of the foreground population. The amplitude of this galaxy-shear correlation function is proportional to Ω_m . Preliminary results from the SDSS for a sample of 30,000 foreground and 1.5 million background galaxies are consistent

with $\Omega_m \simeq 0.2 - 0.3$ [30].

Another probe which constrains a combination of parameters similar to weak lensing is the abundance of galaxy clusters by mass. This abundance is sensitive to the mass power spectrum on cluster scales, and therefore probes σ_8 and Ω_m with a degeneracy similar to that from cosmic shear. Traditionally, X-ray and optical observations have been used to identify clusters and infer their masses. This is now being augmented with weak lensing measurements and Sunyaev-Zel'dovich observations. Each of these techniques has advantages and disadvantages: for X-ray and SZ measurements, one must rely on hydrostatic equilibrium to infer the cluster mass from the X-ray temperature or gas optical depth. For weak lensing, one must worry about other mass along the line of sight, not associated with the cluster, contributing to the shear of background source galaxy images. Fortunately, in a few years we should be in possession of a large sample of clusters which have been probed by these multiple techniques, so that they can be cross-calibrated against each other. At the moment, however, from both clusters and weak lensing there is considerable uncertainty in the cluster-derived value of σ_8 at a given value of Ω_m .

Finally, one should not forget the more traditional measures of the mass density which involve inventorying the mass in known systems. For example, X-ray measurements plus the assumption that the gas is in hydrostatic equilibrium in the cluster potential well allow one to infer the gas to total mass ratio. Combined with simulations which indicate this should be a good estimator of Ω_b/Ω_m and with the BBN or CMB estimates of Ω_b , this provides an estimate of $\Omega_m \simeq 0.2 - 0.4$. Weak lensing mass estimates for clusters have been generally consistent with X-ray masses, at least for systems which appear to be relaxed (no sign of a recent merger).

6 Dark Energy & the Accelerating Universe

In 1998, two groups monitoring the brightness of distant Type Ia supernovae found evidence that the expansion of the Universe is currently accelerating rather than decelerating [31, 32]. If General Relativity is valid, this requires a new form of stress-energy-momentum with negative pressure—now called Dark Energy—characterized by its equation of state, $w = p/\rho$, with $w < -1/3$. A cosmological constant—the energy associated with the vacuum—is the simplest but not the only possibility for dark energy: in this case, $w \equiv -1$.

In fact, we now have two broad lines of evidence for Dark Energy. The first, direct evidence for acceleration comes from the supernovae. Work over the last decade has shown that SN Ia, thought to be white dwarfs accreting mass from a

companion which explode when they reach (or approach) the Chandrasekhar limit, are excellent ‘standardizable’ candles, with a dispersion of about 12% in their peak brightness—that is, their distances can be determined to about 6% accuracy. Another advantage of SNe Ia is that they are about as bright as an entire galaxy when they peak, so they can be observed to large distances. Two groups, the Supernova Cosmology Project [31] and the High-Z Supernova Search [32] used SNe at redshifts $z \sim 0.4 - 0.8$ to measure the luminosity distance $d_L(z)$, which probes the expansion history of the Universe, $H(z)$. These high-redshift SNe were found to be about 25% fainter than would be expected in a decelerating Universe.

The second line of evidence is indirect: the CMB indicates a flat Universe, with $\Omega_{tot} = 1$, while the CMB, large-scale structure, and clusters all point to $\Omega_m = 0.3$, as noted in the previous section. Consequently, there must be a ‘missing energy’ component with $\Omega = 0.7$. In order for large-scale structure to have formed, the missing energy—which does not cluster on galaxy and cluster scales—can only have come to dominate the Universe quite recently. Since the density ρ scales with the cosmic scale factor $a(t)$ as $\rho \sim a^{-3(1+w)}$ ($w = 0$ for ordinary matter), in order to dominate only recently the missing energy must have negative pressure, $w < -0.5$ or so. A similar upper bound on w arises from combining the age of the Universe (from globular clusters or from the CMB) with measurements of the Hubble parameter, which indicate $H_0 t_0 \simeq 1$. Parsimony suggests that we identify the negative-pressure missing energy with the negative-pressure dark energy driving the acceleration.

In fact, an accelerating Universe had been invoked repeatedly throughout the 20th Century, but the evidence always evaporated in the face of more reliable data or improved understanding of systematics. What has changed is that for the first time we now have multiple lines of evidence pointing to dark energy, each subject to different systematic errors. Combining the SNe and CMB results, one again finds the best fit concordance model with $\Omega_m \simeq 0.3$, $\Omega_{DE} \simeq 0.7$. Combining the SN data with large-scale structure measurements, one finds that the dark energy equation of state should satisfy roughly $w < -0.6$ (at 95% CL).

For the supernovae, systematic concerns include the possibility of grey dust causing the distant SNe to appear fainter, possible differences in the SN population between high and low redshift (e.g., due to changes in chemical composition), and issues of photometric calibration, among others. Fortunately, supernovae provide enough information that many of these issues can be addressed with additional observations. For example, with grey dust, one would expect to find SNe look intrinsically fainter at higher redshift, while the serendipitous discovery of SN1997ff in the Hubble Deep Field at $z \sim 1.7$ indicates this is not the case [33]. Moreover,

due to finite grain size, grey dust would not look grey in the infrared; near-IR observations of high-redshift SNe show no signs of the effect. It is also thought that evolution and chemical composition issues can be addressed by comparing low- and high-redshift SNe in similar environments (e.g., elliptical vs. spiral galaxies, etc). The two high- z teams have continued observing high-redshift SNe, particularly obtaining better photometry with the Hubble Space Telescope, and updated results (which confirm the earlier findings) are expected soon. In addition, more ambitious supernova searches aimed at more strongly constraining the dark energy are planned. In the near term, these include the ESSENCE and CFHT Legacy Surveys, and in the long run the SNAP satellite mission.

Moreover, the prospects for developing and maturing new complementary cosmological probes of the dark energy over the next decade appear quite good. These probes have three successive aims: (i) to provide independent direct evidence for acceleration, to confirm the SNe results, (ii) to determine the equation of state w with sufficient precision that the cosmological constant ($w = -1$) can be distinguished from, say, $w = -0.8$, (iii) if $w \neq -1$, to constrain the time evolution of $w(z)$. Since particle physics theory at present provides no guidance about the nature of the dark energy (as indicated by the fact that the vacuum energy is at least 57 orders of magnitude smaller than what one expects in a supersymmetric theory), such experimental progress is needed to point the way forward. These new probes include the Alcock-Paczynski test using the clustering of intermediate redshift galaxies and of the Lyman-alpha forest absorbers; galaxy number counts; the cluster mass function vs. redshift, cosmic shear tomography, and CMB lensing, among others. These probes each make use in different ways of the two observables affected by dark energy, the distance measure as a function of redshift, and the growth rate of density perturbations as a function of redshift.

7 Conclusion

The advent of precision cosmology is bringing more sharply into focus the fundamental physics issues underlying the values of the cosmological parameters. While measurement of the cosmological parameters has been advancing, and has established the standard cosmological model on firm ground, these advances have thrown into sharp relief some key questions for cosmology at the turn of the 21st century:

- Did inflation occur in the early Universe, and did it originate the perturbations that formed large-scale structure?

- What is the nature of the Dark Matter that makes up most of the (non-relativistic) mass of the Universe?
- What is the nature of the Dark Energy that is causing the expansion of the Universe to accelerate?
- Are there more than three spatial dimensions? If so, can we ever detect them?

The continuing expected advances in CMB measurements (MAP and Planck), coupled with the long-term possibility of detecting the gravity-wave induced B-mode of polarization, offer the best hopes for addressing the issue of inflation. On dark matter, direct detection experiments are now beginning to push down into the SUSY model parameter range and they will be augmented by future collider studies. At present, the Dark Energy remains a mystery wrapped in the larger enigma of the cosmological constant. However, new surveys for high-redshift supernovae, coupled with constraints from Planck, offer the hope of precision measurement of w and of plausibly constraining its evolution with redshift. In addition, a number of other dark energy probes, with differing systematic errors and nearly orthogonal parameter degeneracies, are expected to reach maturity over the coming decade. Finally, a topic I have not had time to cover: if the extra dimensions are large, as recent theories incorporating branes make possible, then they could yield signatures at TeV-scale colliders. Large extra dimensions would have dramatic consequences for early Universe cosmology, a topic now in the early days of its exploration.

Acknowledgements

I thank the organizers for arranging and enjoyable conference. Research supported by the DOE at Fermilab and Chicago, by NASA grant NAG5-10842 at Fermilab, by NSF grant PHY-0079251 at Chicago, and by the Center for Cosmological Physics. Since this is based on an informal review talk, the references represent an idiosyncratic subsample (a complete bibliography would have been as long as the paper itself); apologies to those whose work should have been included.

References

1. J. Kovac *et al*, astro-ph/0209478
2. S. Burles, K. Nollett, and M. S. Turner, *Astrophys. J.* **442**, L1 (2001).
3. W. Freedman *et al*, *Astrophys. J.* **553**, 47 (2001).

4. C. Pryke *et al*, *Astrophys. J.* **568**, 46 (2002).
5. C. Netterfield *et al*, *Astrophys. J.* **571**, 604 (2002).
6. A. T. Lee *et al*, *Astrophys. J.* **561**, L1 (2001).
7. For a recent review, see W. Hu and S. Dodelson, *Ann. Rev. Astron. Astrophys.* (2002), in press; astro-ph/0110414
8. A. Lewis and S. Bridle, astro-ph/0205436
9. L. Knox, N. Christensen, and C. Skordis, *Astrophys. J.* **563**, L95 (2001).
10. T. Pearson *et al*, astro-ph/0205388; B. Mason *et al*, astro-ph/0205384
11. J. R. Bond *et al*, astro-ph/0205386
12. M. Kamionkowski, A. Kosowsky, and A. Stebbins, *Phys. Rev. Lett.* **78**, 2058 (1997).
13. M. Zaldarriaga, D. Spergel, and U. Seljak, *Astrophys. J.* **488**, 1 (1997).
14. E. Gaztanaga and J. Frieman, *Astrophys. J.* **437**, L13 (1994); J. Frieman and E. Gaztanaga, *Astrophys. J.* **521**, 83 (1999).
15. L. Verde *et al*, astro-ph/0112161
16. O. Lahav *et al*, astro-ph/0112162
17. P. Norberg *et al*, astro-ph/0112043
18. I. Zehavi *et al*, *Astrophys. J.* **571**, 172 (2002).
19. W. Percival *et al*, astro-ph/0105252
20. A. Szalay *et al*, astro-ph/0107419; S. Dodelson *et al*, *Astrophys. J.* **572**, 140 (2001); M. Tegmark *et al*, *Astrophys. J.* **571**, 191 (2002); A. Connolly *et al*, astro-ph/0107417; R. Scranton *et al*, astro-ph/0107416
21. J. Peacock *et al*, *Nature* **410**, 169 (2001).
22. M. Strauss and J. Willick, *Phys. Rept.* **261**, 271 (1995).
23. S. Zaroubi, E. Branchini, Y. Hoffman, and L. da Costa, astro-ph/0207356

24. D. Wittman *et al*, Nature **405**, 143 (2000).
25. L. van Waerbeke *et al*, astro-ph/0002500
26. D. Bacon *et al*, astro-ph/0003008
27. H. Hoekstra *et al*, astro-ph/0202285
28. N. Kaiser, G. Wilson, and G. Luppino, astro-ph/0003338
29. A. Refregier, J. Rhodes, and E. Groth, astro-ph/0203131
30. P. Fischer *et al*, Astron. J. **120**, 1198 (2000).
31. S. Perlmutter *et al*, Astrophys. J. **517**, 565 (1999).
32. A. Riess *et al*, Astron. J. **116**, 1009 (1998).
33. A. Riess *et al*, Astrophys. J. **560**, 49 (2001).

Disclaimer

Operated by Universities Research Association Inc. under
Contract No. DE-AC02-76CH03000 with the United States Department of Energy.

This report was prepared as an account of work sponsored by an agency of the United States Government. Neither the United States Government nor any agency thereof, nor any of their employees, makes any warranty, express or implied, or assumes any legal liability or responsibility for the accuracy, completeness, or usefulness of any information, apparatus, product, or process disclosed, or represents that its use would not infringe privately owned rights. Reference herein to any specific commercial product, process, or service by trade name, trademark, manufacturer, or otherwise, does not necessarily constitute or imply its endorsement, recommendation, or favoring by the United States Government or any agency thereof. The views and opinions of authors expressed herein do not necessarily state or reflect those of the United States Government or any agency thereof.

Approved for public release; further dissemination unlimited.